FOUGERITE, A NEW MINERAL OF THE PYROAURITE-IOWAITE GROUP: DESCRIPTION AND CRYSTAL STRUCTURE

Fabienne Trolard[1],*, Guilhem Bourrié[1], Mustapha Abdelmoula[2], Philippe Refait[3] and Frédéric Feder[4]

[1] INRA, UR1119, Géochimie des Sols et des Eaux, F-13545 Aix-en-Provence, France
[2] Université Henri Poincaré − Nancy I, UMR CNRS 7564, Laboratoire de Chimie Physique et Microbiologie pour l'Environnement, 405 rue de Vandœuvre, F-56400 Villers-lès-Nancy, France
[3] LEMMA, Université de La Rochelle, Bâtiment Marie Curie, Av. Michel Crépeau, F-17042 La Rochelle cedex 01, France
[4] CIRAD, internal research unit 'Environmental Risks of Recycling', Station de la Bretagne, BP 20, F-97408 Saint-Denis messagerie Cedex, Réunion, France

Abstract—Fougerite (IMA 2003-057) is a mixed M(II)-M(III) hydroxysalt of the green rust group, where M(II) can be Fe or Mg, and M(III) is Fe. The general structural formula is: $[Fe_{1-x}^{2+}Fe_x^{3+}Mg_y(OH)_{2+2y}]^{+x}[x/n A^{-n}.mH_2O]^{-x}$ where A is the interlayer anion and n its valency, with $1/4 \leqslant x/(1+y) \leqslant 1/3$ and $m \leqslant (1-x+y)$. The structure of green rusts and parent minerals can accommodate a variety of anions, such as OH^-, Cl^-, CO_3^{2-}, SO_4^{2-}. The structure of the mineral was studied by Mössbauer, Raman and X-ray absorption spectroscopies (XAS) at the FeK edge. Mössbauer spectra of the mineral obtained at 78 K are best fitted with four doublets: D1 and D2 due to Fe^{2+} (isomer shift $\delta \approx 1.27$ and 1.25 mm s^{-1}, quadrupole splitting $\Delta E_Q \approx 2.86$ and 2.48 mm s^{-1}, respectively) and D3 and D4 due to Fe^{3+} ($\delta \approx 0.46$ mm s^{-1}, $\Delta E_Q \approx 0.48$ and 0.97 mm s^{-1}, respectively). Microprobe Raman spectra obtained with a laser at 514.53 nm show the characteristic bands of synthetic green rusts at 427 and 518 cm^{-1}. X-ray absorption spectroscopy shows that Mg is present in the mineral in addition to Fe, that the space group is $R\bar{3}m$ and the lattice parameter $a \approx 0.30-0.32$ nm. The mineral forms by partial oxidation and hydrolysis of aqueous Fe^{2+}, to give small crystals (400−500 nm) in the form of hexagonal plates. The mineral is unstable in air and transforms to lepidocrocite or goethite. The name is for the locality of the occurrence, a forested Gleysol near Fougères, Brittany, France. Its characteristic blue-green color (5BG6/1 in the Munsell system) has long been used as a universal criterion in soil classification to identify Gleysols. From a thermodynamic model of soil-solution equilibria, it was proposed that for the eponymous mineral, *Fougères*-fougerite, OH^- may be the interlayer anion. In other environments, the interlayer anion may be different, and other varieties of fougerite may exist. Fougerite plays a key role in the pathways of formation of Fe oxides.

Key Words—Fe, Fougerite, Gleysol, Green Rust, Hydroxide, Iowaite, Mg, New Mineral, Pyroaurite, Soil.

INTRODUCTION

The blue-green colors in sediments and hydromorphic soils that turn ochreous on contact with air have long been assumed to result from the presence of mixed-valence Fe(II)-Fe(III) compounds (Vysotskii, 1905 [1999]; Ponnamperuma *et al.*, 1967; Nguyen Kha and Duchaufour, 1969; Avery, 1973; Duchaufour *et al.*, 1976; Taylor, 1981, 1984). In synthesis experiments, Girard and Chaudron (1935) observed the precipitation of a metastable 'green oxide' that transformed into lepidocrocite by oxidation and named it "hydrated magnetite" with the tentative formula $Fe_3O_4.nH_2O$. Later, Feitknecht and Keller (1950) and Bernal *et al.* (1959) synthesized similar compounds and gave them the generic name "green rusts". Many authors proposed that they were part of the pyroaurite-sjögrenite group and consisted of brucite-like sheets carrying a positive charge alternating with layers comprising anions and water molecules, a structure close to that of pyroaurite (Allmann, 1968, 1970; Taylor, 1973; Brindley and Bish, 1976; Bish and Brindley, 1977; Brindley and Kikkawa, 1979; Hashi *et al.*, 1983). These compounds were distinguished by their X-ray diffraction (XRD) patterns, as green rust one (GR1), and green rust two (GR2) (Bernal *et al.*, 1959). GR1 forms with planar or spherical anions such as carbonate, chloride, oxalate; in this group, layers are separated by only one layer of water molecules, and the sequence of stacking of OH planes along the c axis is $ABBCCA$; GR2 forms with tetrahedral anions, such as sulfate and selenate; in this group, layers are separated by two layers of water molecules and the sequence of OH planes is ABA (Simon *et al.*, 2003). Green rusts (GRs) were first observed in corrosion products of steel (Stampfl, 1969; Bigham and Tuovinen, 1985; Al-Agha *et al.*, 1995), then in a waste sludge (Koch and Mørup, 1991), and finally recognized in soils (Trolard *et al.*, 1996, 1997; Feder *et al.*, 2005). Fougerite has been approved as a new mineral by the International Mineralogical Association (IMA) with the number

* E-mail address of corresponding author:
trolard@aix.inra.fr

323

2003−057, and the name has also been approved by the IMA.

The objectives of this paper are threefold: (1) to summarize the main results obtained on the characterization of fougerite, as a reference paper requested by IMA; (2) to collect new data, obtained on soil samples from Fougères, by selective dissolution techniques, in order to constrain better the composition of fougerite; and (3) to establish the geochemical implications of the existence of fougerite on the pathways of formation of Fe oxides.

OCCURRENCE

The mineral occurred in a subsurface horizon of a Gleysol showing a reductomorphic color pattern (Gr) (IUSS Working Group WRB, 2006), formed on a granitic saprolite. It was sampled first at 15−30 cm depth (Figure 1) in a forest near the city of Fougères, France. The exact coordinates of the sampling point in the Lambert I system IGN are 3400103 and 81634.

The fougerite formed by partial oxidation and hydrolysis of aqueous Fe^{2+}. Associated minerals were weathering products, either newly formed or residual, of a granodiorite and included kaolinite, vermiculite, quartz, illite and feldspars.

Alteration

The mineral transformed easily by oxidation into Fe^{3+} oxides (lepidocrocite, goethite) and this transformation was accompanied by a color change of the sample from blue to ochre. Thus the sample was collected in a large volume with the surrounding soil solution and maintained under anoxic conditions in an airtight box without sieving or air-drying. The permanence of the original blue or blue-green colors during all experiments was used as a preservation criterion.

APPEARANCE AND PHYSICAL PROPERTIES

The fougerite crystals were very small (~400−500 nm) and were dispersed throughout the sample. They occurred as hexagonal particles with a tabular morphology similar to kaolinite (Figure 2). The color was an homogeneous bluish-gray (5BG6/1) that turned after about 10 minutes in air to a greenish-gray (5GY6/1), then to pale-olive (5Y6/4) after 1 h, and eventually to gray with light-olive spots (2.5Y5/6) after one day's exposure. The mineral showed no fluorescence.

No other physical data were collected due to the nature of the sample.

MÖSSBAUER AND RAMAN IDENTIFICATION

Fougerite was identified by Mössbauer and Raman spectroscopies. The parameters for the mineral were obtained by calibration of the methods using synthetic green rusts.

Mössbauer spectroscopy

Methods. Transmission Mössbauer spectroscopy (TMS) measurements were done at 77±1 K on materials taken from the core of the oversized sample and introduced to the cryostat (Cryo Industries of America) where they were sheltered from oxygen. Mössbauer spectra were accumulated with a constant-acceleration spectrometer and a 512 multichannel analyzer (Halder Elektronic Gmbh), with a 50 mCi source of ^{57}Co in Rh maintained at room temperature. The velocity was calibrated with a 25 μm foil of α-Fe at room temperature, and the isomer shifts were derived with respect to this reference. The amount of material was optimized to ~10 mg of Fe per cm^2. The spectra of fougerite were similar to those of synthetic 'green rusts' (Trolard *et al.*, 1996, 1997; Génin *et al.*, 1998; Feder *et al.*, 2005), and were best

Figure 1. Type locality at Fougères: soil profile with blue-green Gr horizon containing fougerite. At the surface, litter made of beech leaves, overlying an organo-mineral horizon (0−15 cm) and the horizon showing gleyic, specifically reductomorphic properties Gr (15−30 cm). The groundwater table can be seen at the bottom of the profile.
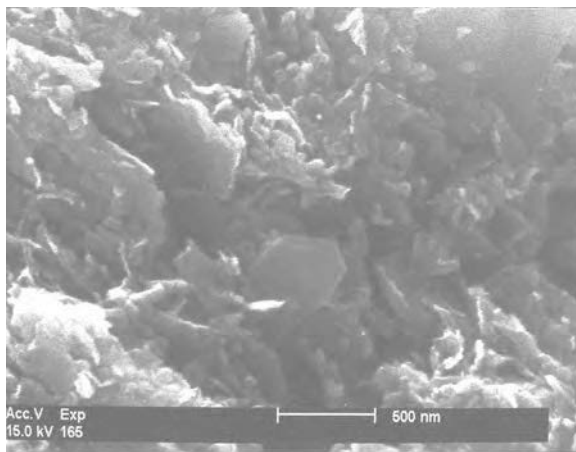

Figure 2. SEM image of fougerite particles (hexagonal crystals); particle size is ~500 nm.

approximated by a sum of lines with Lorentzian shape (thin-absorber approximation) and small linewidths of about 0.3 mm s^{-1} (Refait *et al.*, 2001).

Results. The first spectrum on a sample taken at 20 cm depth and obtained by classical transmission spectroscopy at 77−78 K could be fitted with only two doublets: D1 (isomer shift δ = 1.25 mm s^{-1} and quadrupole splitting ΔE_Q = 2.87 mm s^{-1}) and D3 (δ = 0.45 mm s^{-1} and ΔE_Q = 0.54 mm s^{-1}). The doublet D1 was ascribed to Fe^{2+} and D3 to Fe^{3+}. Three other samples taken later at 20, 40 and 60 cm gave similar results for D1 (δ = 1.25 mm s^{-1} and ΔE_Q = 2.81, 2.81 and 2.88 mm s^{-1}) and D3 (δ = 0.43, 0.44 and 0.45 mm s^{-1} and ΔE_Q = 0.72, 0.61 and 0.58 mm s^{-1}) (Abdelmoula *et al.*, 1998). The positions of the D1 and D3 doublets were thus very close to the values obtained for synthetic green rusts D1 (δ = 1.27 mm s^{-1} and ΔE_Q = 2.87−2.92 mm s^{-1}), D3 (δ = 0.47−0.48 mm s^{-1} and ΔE_Q = 0.38−0.43 mm s^{-1}), and conform with the observation that Fe^{2+} in synthetic green rusts has a very constant, oxidation-insensitive ΔE_Q = 2.8 mm s^{-1} (Murad and Taylor, 1986). A distinct ferric doublet D′3 (δ = 0.53 mm s^{-1} and ΔE_Q = 0.55 mm s^{-1}), observed at the 60 cm level was ascribed to lepidocrocite (Abdelmoula *et al.*, 1998). This last sample was yellowish, while the other three samples showed the typical bluish-green color characteristic of gleys. More recently, and by comparison with synthetic Mg-Fe(II)-Fe(III) pyroaurites, four doublets were fitted to the spectrum obtained at 78 K on another sample taken in the same profile, at 90 cm: two ferrous doublets, D1 (δ = 1.27 mm s^{-1} and ΔE_Q = 2.86 mm s^{-1}) and D2 (δ = 1.27 mm s^{-1} and ΔE_Q = 2.48 mm s^{-1}) and two ferric doublets, D3 (δ = 0.46 mm s^{-1} and ΔE_Q = 0.48 mm s^{-1}) and D4 (δ = 0.46 mm s^{-1} and ΔE_Q = 0.97 mm s^{-1}) (Refait *et al.*, 2001). The second ferrous doublet D2 is observed when the structure is GR1 and the space group is $R\bar{3}m$ (Refait *et al.*, 1998a, 1998b). It is ascribed to Fe(II) cations close to the interlayer anions. The presence of ferrous doublets clearly separates green rusts and fougerite from superparamagnetic Fe(III) oxides. When silicated Fe is present, and if Fe is present both as Fe(II) and Fe(III) in the octahedral sheet of clay minerals, the distinction may be difficult. By plotting δ *vs.* ΔE_Q, the points for fougerite appear distinct from the points for clay minerals (Feder *et al.*, 2005), but selective dissolution must be used to estimate the fraction of silicated Fe (see lower).

Raman spectroscopy

Methods. In order to confirm the identification of the mineral, a Raman characterization was performed. A special cell allowed us to keep the sample in nitrogen or argon atmosphere. In a glove box, under argon atmosphere, the cell was closed tightly with a glass window through which a laser beam was focused and the Raman backscattering collected. The cell was mounted in the focal plane of an Olympus B.H. microprobe in a Jobin-Yvon/Instrument S.A. T64000 Raman microprobe equipped with a charged coupled device detector and an X-Y motorized stage. A large working distance objective length of 50× magnification was used. Thus, the laser at a wavelength of 514.53 nm was focused on an area of ~2 μm diameter with a power of <1 mW to prevent sample degradation.

Results. A Raman spectrum acquired on the first sample (Trolard *et al.*, 1997) showed the same characteristic bands at 427 and 518 cm^{-1} as synthetic green rusts (Boucherit *et al.*, 1991, 1992). However, due to the small concentration of fougerite in the natural soil sample, the Raman spectra did not allow us to determine the nature of the interlayer anion.

OPTICAL PROPERTIES

No data were collected due to the nature of the material.

CRYSTALLOGRAPHY AND CHEMICAL COMPOSITION OF THE MINERAL

The structure of the mineral was studied by extended X-ray absorption fine structure spectroscopy (EXAFS), which showed that it belongs to the pyroaurite group, but showed too that it contains Mg in addition to Fe, unlike synthetic green rusts. This result was confirmed by electron microprobe analyses and selective extraction techniques.

Assumed structure on the basis of XRD data on synthetic green rusts and pyroaurites and EXAFS measurements on fougerite

The structure of fougerite was believed to be that of GR1(OH), but GR1(OH) has until now never been synthesized. From a structural point of view, GR1(OH) should be very similar to GR1(Cl). The structure of a synthetic GR1(Cl) was investigated by XRD (Refait *et al.*, 1998a) and proved to be almost identical to that of iowaite, a Mg(II)-Fe(III) mineral (Braithwaite *et al.*, 1994). Iowaite has a structure similar to pyroaurite, a Mg(II)-Fe(III) hydroxycarbonate, except that the interlayer charge balance is maintained by Cl$^-$ ions instead of CO_3^{2-}. The XRD data, reduced co-ordinates of atoms, interatomic distances and temperature factors for GR1(Cl) according to Refait *et al.* (1998a) are compiled in Tables 1, 2 and 3.

A structural model for GR1(OH) was thus proposed by Génin *et al.* (2001), derived from that of GR1(Cl) (Refait *et al.*, 1998a). The basic principle is that anions of Cl$^-$ or OH$^-$ balance the positive charges of the hydroxide sheets and are isolated from each other in the interlayers by water molecules. Due to the disordered

Table 1. XRD data (CoKα_1 radiation) compared with computed interplanar distances (nm) and intensities of synthetic GR1(Cl); from Refait *et al.* (1998a). The structure is $R\bar{3}m$ with parameters $a = 0.3190(1)$ nm and $c = 2.385(6)$ nm ($V = 0.2102$ nm^3).

hkl	d_{obs}	d_{calc}	$d_{obs}-d_{calc}$	I_{obs}/I_1	I_{calc}/I_1	I_{obs}/I_{calc}
003	0.797 (3)	0.7950	0.002	100	100	1
006	0.3966 (8)	0.3975	−0.0009	31.5	31.5	1
101	0.2744 (6)	0.2744	0			
012	0.2692 (4)	0.2691	0.0001	34	30.8	1.104
009	0.264 (1)	0.2650	−0.001			
104	0.253 (2)	0.2507	−0.0023	4.5	5.4	0.833
015	0.2392 (3)	0.2391	0.0001	21	21.5	0.977
107	0.216 (2)	0.2146	0.0014	2	3.0	0.666
018	0.2027 (3)	0.2026	0.0001	19.2	21.4	0.897
00$\bar{1}$2	0.198 (1)	0.1988	−0.0008			
101$\bar{0}$	0.1808 (4)	0.1805	0.0003	5.5	6.3	0.873
01$\bar{1}$1	0.1702 (5)	0.1706	−0.0004	4.5	6.1	0.738
110	0.1595 (1)	0.1595	0	9.0	8.7	1.034
113	0.1563 (1)	0.1564	−0.0001	10.4	11.3	0.920
10$\bar{1}$3	0.1526 (7)	0.1528	−0.0002	5	3.9	1.282
116	0.1479 (1)	0.1480	−0.0001	4.3	5.9	0.729
01$\bar{1}$4	0.1448 (3)	0.1450	−0.0002	3	2.6	1.154
021	0.1375 (3)	0.1379	−0.0004			
202	0.1364 (2)	0.1372	−0.0008	5	5.3	0.943
024	0.1348 (3)	0.1346	0.0002	1.5	0.8	1.875
205/00$\bar{1}$8	0.1323 (3)	0.1326	−0.0003	6	6.2	0.968
10$\bar{1}$6	0.1309 (4)	0.1312	−0.0003			
027	0.1284 (2)	0.1280	0.0004	0.5	0.8	0.625
208/01$\bar{1}$7	0.1251 (2)	0.1252	−0.0001	5	3.8	1.316
11$\bar{1}$2	0.1240 (3)	0.1244	−0.0004			
Weighted average			+0.0001			1.002

The digits in parentheses are the one-standard-deviation uncertainty in the last digits of the given value.

nature of such interlayers, vacancies are likely to be found. Figure 3 represents the arrangement of OH$^-$ ions and water molecules in GR1(OH) with a formula close to [Fe$_3^{II}$Fe^{III}(OH)$_8$]$^+$[OH,2H$_2$O]$^-$.

The lattice parameter, a, of GRs depends mainly on the Fe(II)/Fe(III) ratio. For instance, the parameter a of GR1(Cl) is equal to 0.319 nm for Fe(II)/Fe(III) $\approx$ 3 (Refait *et al.*, 1998a) and $\approx$0.303 nm for Fe(II)/Fe(III) = 0 (Refait *et al.*, 2003). For a Mg(II)-containing compound, it would depend on the Fe/Mg ratio. An a value of 0.311 nm has been reported for pyroaurite, a Mg(II)-Fe(III) hydroxy-carbonate (Allmann, 1968), as compared to 0.316 nm for GR(CO$_3^{2-}$) (Drissi *et al.*, 1995). Accordingly, the a parameter of Mg(II)-Fe(II)-Fe(III) hydroxycarbonates, determined from XRD analyses, was found to be intermediate between that of pyroaurite and that of GR(CO$_3^{2-}$) (Refait *et al.*, 2001). It was, for instance,

measured at $a = 0.3126 \pm 0.0005$ nm for the compound [Fe$_2^{II}$Mg$_2^{II}$Fe$_2^{III}$(OH)$_{12}$]$^{2+}$[CO$_3$,nH$_2$O]$^{2-}$. A value of $a = 0.3125 \pm 0.0005$ nm was determined from EXAFS measurements of fougerite (Refait *et al.*, 2001).

The lattice parameter, c, of GR1 compounds is mainly determined by the geometry and size of the interlayer anion (see Figure 3a for instance). It is $c \approx 2.385$ nm in GR1(Cl) (Refait *et al.*, 1998a) and c $\approx$ 2.256 nm in GR1(CO$_3$) (Drissi *et al.*, 1995; Abdelmoula *et al.*, 1996). In GR1(CO$_3$), the carbonate ions are parallel to the hydroxide sheets and the width of the interlayer is fixed by the diameter of the oxygen atoms of H$_2$O and CO$_3^{2-}$. Thus, the parameter c of GR1(OH) should be in the range between that of GR1(Cl) and of GR1(CO$_3$), *i.e.* $c \approx$ [2.256, 2.385] nm. However, it is not accessible by extended X-ray absorption fine structure (EXAFS) spectroscopy which probes only the local environment

Table 2. Reduced coordinates of atoms in synthetic GR1(Cl) and temperature factor.

	x	y	z	U_{11}	U_{22}	U_{33}	U_{23}	U_{13}	U_{12}
Fe	0	0	0	0.009	0.009	0.025	0	0	0.0045
O (OH)	0	0	0.375	0.014	0.014	0.06	0	0	0.007
O (H$_2$O)	0.1	0.1	0.5	0.15	0.15	0.08	0.02	-0.02	0.1
Cl	0.25	0.25	0.5	0.3	0.3	0.08	0.02	-0.02	0.1

Table 3. Layer to layer and interatomic distances in synthetic GR1(Cl) (nm).

Layer to layer distances		
Fe−OH: 0.099	OH−OH in hydroxide sheet: 0.199	OH−interlayer: 0.298
Interatomic distances		
Fe−OH: 0.209	OH−OH (6×): 0.319	OH−OH (3×): 0.277
OH−H₂O: 0.300	OH−Cl: 0.309	Cl−H₂O (min.): 0.320

of the target nucleus and for Fe only sees the arrangement of metals in the (a,b) plane. The EXAFS spectroscopy of selenate-green rust, $GR2(SeO_4)$ at the SeK edge showed only that Se is surrounded by O in tetrahedral coordination and did not yield information on the interaction of the anion with the layer.

Electron microprobe

Electron microprobe analyses (40) were performed on three samples from Fougères, of which 32 (Table 4) showed the presence of Fe, each point being the average analysis of 2 μm³. They showed that Mg_{total}/Fe_{total} mole ratios ranged from 0.18 to 0.62. Measurements compromised two factors: (1) the size of the crystals, ~500 nm, was at the lower limit of the microprobe method; (2) the mineral could not be separated from other constituents without destruction, as it was more labile than the associated minerals.

Selective chemical extractions

Selective extraction techniques using citrate-bicarbonate (CB) and dithionite-citrate-bicarbonate − (DCB) (Trolard *et al.*, 1995 and this study) give additional information. Fougerite is labile, and kinetic extractions of Fe by CB in a nitrogen atmosphere showed that fougerite, just like synthetic green rusts (Trolard *et al.*, 1996), dissolves completely in a few hours, whereas goethite and lepidocrocite are not dissolved by CB, but by DCB. Silicated Fe is not dissolved by either of those reagents (Mitchell *et al.*, 1971). To estimate the proportion of silicated Fe better and to confirm the presence of Mg in fougerite, as suggested earlier by XAS, selective dissolutions were made on soil samples in Fougères. The positions of the samples in the profile are given in Table 5 and the results of selective extractions are given in Table 6.

The results show that silicated Fe in Fougères amounts to 5−14% of total Fe, and CB-extractable Fe to 22 to 60% of total Fe. Clearly, reductive conditions in Gleysols destabilize silicated Fe, and clay minerals are mainly aluminous. This is in agreement with previous results obtained by Aurousseau *et al.* (1987) and with the results obtained by XRD (not shown here): in Fougères, the clay minerals consist mainly of kaolinite, hydroxy-Al vermiculite, close to an Al-beidellite and illite.

In the reductomorphic silty horizon at Fougères, 59% of the total Mg was extracted by CB, and Mg and Fe were simultaneously released over time. The kinetics obtained were: Fe/Mg = 0.5981 + 0.000792 t, (r^2 = 0.975, N = 4). The intercept was Fe/Mg = 0.5981, which corresponds to a global Mg/Fe value equal to 1.67. We can thus conclude that Mg present in the CB-extractable compartment was associated with Fe, *i.e.* originated from fougerite. In the reductomorphic saprolite, 48% of the Mg was extractable by CB, and all this Mg was extracted in 6 h, with the global mole ratio (Mg/Fe)$_{CB}$ being close to 1. No additional Mg was extracted by DCB. These results show that Mg is present both in the silicate phase (41 to 52%) and in fougerite (48−59%) but not in well crystallized Fe oxides. The values obtained for the global mole ratio by selective extraction techniques are thus in the range 0.1−1.7. This range is compatible with the local mole ratio obtained by XAS.

In the oximorphic saprolite, the pattern was different. Though 57% of total Mg was released by CB or DCB, only 22% of total Fe was released by CB. In that
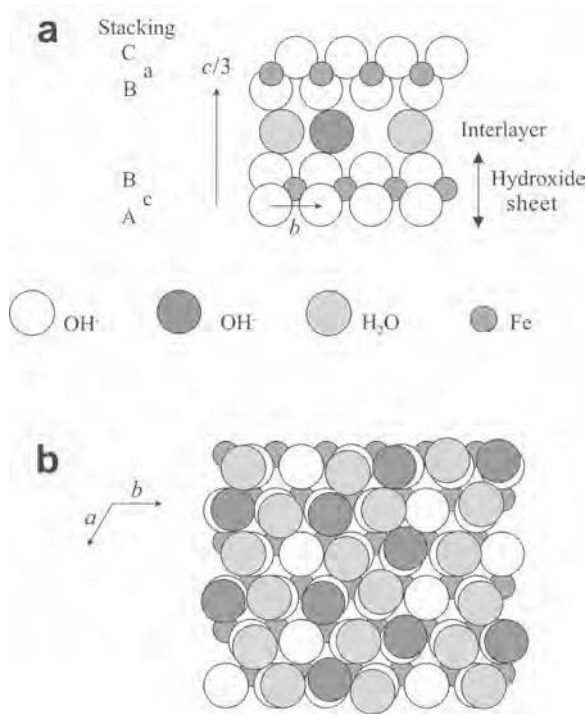

Figure 3. Proposed crystal structure of GR1(OH) for a chemical composition of $[Fe_3^{II}Fe^{III}(OH)_8]^+$ $[OH, 2H_2O]^−$. (a) Stacking sequence; (b) positions of water molecules and OH− ions in an interlayer viewed along [001]. Relative sizes of ions are drawn to scale. One interlayer, one OH plane and one Fe plane are represented below.

Table 4. Microprobe analyses on the clay particles from Fougères'site. The volume analyzed is ~1 μm^3, and thus larger than the particle size.

No	Fe K	Mg K	O K	Si K	Al K	K K	Na K
1	3.22	1.69	71.78	9.45	6.93	0.42	
2	4.58	2.44	72.43	9.04	6.74	n.d.	
3	2.97	1.67	71.3	10.94	7.36	0.46	
4	3.74	1.9	70.45	10.82	7.39	0.3	
6	5.27	2.23	71.07	10.53	6.52	0.3	
7	6.28	2.63	68.52	11.16	7.15	n.d.	
8	2.22	1.09	70.87	11.16	7.83	0.62	
9	1.58	0.8	61.91	17.71	10.2	1.74	
11	4.64	3.18	73.36	8.09	6.43	n.d.	
12	5.4	2.97	75.75	9.17	6.71	n.d.	
13	5.13	2.95	76.49	9.01	6.42	n.d.	
14	5.4	3.16	69.5	10.12	7.68	n.d.	
15	7.66	2.89	63.94	11.06	8.29	0.66	
16	0	0.75	68.24	13.86	10.64	1.04	
17	0	0	75.26	11.21	9.27	n.d.	
18	1.38	1.58	69.11	12.18	8.86	1.54	
19	0	0	72.89	20.27	2.54	0.42	
20	1.95	1.35	68.79	12.56	9.35	0.69	
21	4.1	2.57	74.67	8.61	6.24	n.d.	0.675
22	0.68	0.33	70.21	12.03	9.62	1.86	
23	2.81	1.69	73.7	10.17	7.99	n.d.	
24	0	0	59.53	17.45	13.8	4.32	
25	0	0	55.24	20.52	16.64	n.d.	
26	5.33	3.04	69.61	10.04	7.43	n.d.	
27	3.58	1.41	71.11	12.6	9.46	1.59	
28	5.3	3.03	73.32	10.28	7.66	0.41	1.43
29	6.02	3.44	68.32	10.06	7.44	n.d.	1.56
30	4.75	2.07	70.92	9.24	6.95	0.31	
31	5.43	3.66	70.35	9.06	7.35	n.d.	
32	0	1.06	53.33	21.57	13.35	2.37	

n.d. not determined

horizon, at that time, a large part of Mg was probably present on exchangeable sites. For all samples, the quantities of Al and Si extracted by CB and DCB are similar and small and can be ascribed to a small dissolution of clay minerals and of interlayer Al.

NAME

The name is for the site where the mineral was first characterized, a forest near Fougères, Brittany, France. We did not choose the name of a person because for the last 70 y many people have been working on the

Table 5. Nature of soil samples from Fougères studied by selective dissolution (Feder, 2001).

No	Horizon/Gleyic color pattern	Depth (cm)
1	Oximorphic silty	20
2	Oximorphic silty	40
3	Reductomorphic silty	60
4	Reductomorphic saprolite	80
5	Oximorphic saprolite	100

structure and stabilization of the synthetic forms but have failed to find the phase in nature.

TYPE MATERIAL

Though it is stable in its conditions of formation, fougerite is unstable in air; thus, a fougerite sample could not be deposited permanently in a museum. It can be maintained in the laboratory under anoxic conditions in a container for a period of several months.

DISCUSSION

Structural formula and composition

The proposed structural formula for fougerite is:

$[Fe^{2+}_{1-x}Fe^{3+}_x Mg_y(OH)_{2+2y}]^{+x}[x/n\ A^{-n}\ mH_2O]^{-x}$, with $1/4 \leqslant x/(1+y) \leqslant 1/3$, where A is the anion and n its valency. With this formula, $Z = 3$.

The structural formula is derived from the following results:

(1) Direct measurements by Mössbauer spectrometry, both in the laboratory and *in situ* in the field, showed that x ranges from 1/3 to 2/3. The determination of the

Table 6. Results of selective dissolution by citrate-bicarbonate (CB) and dithionite-citrate-bicarbonate (DCB): mole ratios of elements extracted after 500 h.

Sample/CB extraction	Fe_{CB}/Fe_{total}	Mg_{CB}/Mg_{total}	Si_{CB}/Si_{total}	Al_{CB}/Al_{total}
3 Reductomorphic silty	0.60	0.59	0.012	0.26
4 Reductomorphic saprolite	0.57	0.48	0.013	0.15
5 Oximorphic saprolite	0.22	0.57	0.019	0.04

Sample/DCB extraction	Fe_{DCB}/Fe_{total}	Mg_{DCB}/Mg_{total}	Si_{DCB}/Si_{total}	Al_{DCB}/Al_{total}
3 Reductomorphic silty	0.95	0.56	0.03	0.27
4 Reductomorphic saprolite	0.86	0.54	0.02	0.20
5 Oximorphic saprolite	0.94	0.58	0.05	0.27

Mössbauer spectral parameters was estimated to ±0.02 mm s^{-1} by analyzing three samples, with the precision of x of ~0.01.

(2) Both Fe^{2+} and Fe^{3+} valence states occur in close proximity, as shown by X-ray absorption near edge spectroscopy (XANES) (Refait *et al.*, 2001), which is sensitive to the oxidation state of Fe and to its local symmetry; there are no clusters of Fe^{2+} or Fe^{3+}. The mineral was confirmed to be a green rust, a double layered hydroxide, because its pseudo radial distribution function (PRDF) displayed the same set of peaks (P_1−P_6) and was in agreement with a previous study on similar compounds (Roussel *et al.*, 2000). The lattice parameter a was determined to be ~0.31−0.32 nm, as predicted previously, from the second P_2 peak of PDRF, *i.e.* the Fe−Fe distance. The positions of further, and smaller, peaks of the PDRF corresponded to the hexagonal array of cations, second, third... neighbors of Fe, in the sequence $a\sqrt{3}$, $2a$, $a\sqrt{7}$, $3a$...

(3) Mg substitutes for Fe in the mineral. Evidence for this was that the radial distribution function obtained for the mineral was intermediate between those of GR1 and of synthetic pyroaurite, *i.e.* between Fe^{2+}−Fe^{3+} and Mg^{2+}−Fe^{3+} hydroxycarbonates. The peak intensities observed for the mineral were different from the peak intensities of synthetic GRs and intermediate between those of GR1s and synthetic pyroaurite. This was not surprising as many natural minerals are mixed Fe(II)-Mg(II) compounds (pyroxenes, micas, amphiboles, clay minerals...).

(4) The local ratio of Mg/Fe is ~2±1. This was estimated by fitting a linear combination of the contributions of Mg and Fe to the back Fourier transforms of the PRDF curve. In the case of synthetic GR1s, no Mg was present and backscattering atoms were Fe atoms, whereas in synthetic pyroaurite each Fe atom was surrounded by Mg atoms, so that Mg atoms were the only backscattering atoms. A much better fit was obtained when provision was made for Mg and Fe contributions than with only a Fe contribution.

(5) Selective chemical extractions by dithionite-citrate-bicarbonate (DCB) and citrate-bicarbonate (CB) reagents showed that Mg was released proportionally to Fe.

(6) The structural constraint that every Fe^{3+} must be surrounded by 6 bivalent cations, either Fe^{2+} or Mg^{2+}, led to the inequality $x/(1+y) \leqslant 1/3$.

(7) Experimental evidence from syntheses of 'green rusts' showed that they form preferentially when $x/(1+y) \geqslant 1/4$.

(8) Accordingly, fougerite can be considered as a true solid-solution in the system $Mg(OH)_2$-$Fe(OH)_2$-$Fe(OH)_3$ but this solid-solution is not an ideal one, its composition being restricted by the inequalities $1/4 \leqslant x/(1+y) \leqslant 1/3$ (narrow band between dashed line and solid line, Figure 4a). The end-member $Fe(OH)_3$, with a GR structure is virtual. The Gibbs free energy of formation of any fougerite with OH^-, Cl^-, CO_3^{2-}/HCO_3^- or SO_4^{2-} as interlayer anion can be computed from the regular solid-solution model developed previously (Bourrié *et al.*, 2004; Feder *et al.*, 2005).

(9) The nature of the interlayer anion is *a priori* variable, as the structure of green rusts and of parent minerals can accommodate spherical anions, including OH^- and Cl^-, or planar anions such as CO_3^{2-}, and large tetrahedral anions such as SO_4^{2-}, or SeO_4^{2-}. Although in the detail, in this latter case, the structure is different, the generic name fougerite was proposed for the mineral with the structural formula given above with *A* as the interlayer anion. Similarly to hydroxy-apatite, fluoro-apatite and carbonate-apatite, we propose to use hydroxy-fougerite, chloro-fougerite, carbonate-fougerite and sulfate-fougerite to specify the variety when the anion is known. Though selectivity exists, mixing of anions in the interlayer is *a priori* possible, as for smectites. This means that the composition of the layer is considered as more characteristic of the mineral than the composition of the interlayer. Similarly, we propose to use *Fougères*-fougerite, to specify the occurrence, as we use *Montmorillon*-montmorillonite or *Wyoming*-montmorillonite.

(10) The number of moles of water in the interlayer is restricted by the steric hindrance, and for GR1 $m \leqslant 1-x+y$. The maximum number is *a priori* observed with the smaller anion, *i.e.* in the order $OH^- > Cl^- > CO_3^{2-}$. It is larger for GR2. In the case of sulfate-fougerite, the

structure can be GR2, with two layers of water molecules, but sulfate-hydrotalcite and sulfate-pyroaurite were observed with only one interlayer plane, so both structures are *a priori* possible (Simon *et al.*, 2003).

Limits of the composition of Fougères-*fougerite*

The control of dissolved Fe by fougerite in solutions bearing very small concentrations of Cl^- and carbonate (acid conditions, $[CO_3^{2-}] \approx 10^{-10}$ M) suggested that these anions were not likely to be found in the interlayers of the GR of Fougères, because solutions were largely undersaturated with respect to Cl^- and CO_3^{2-} members of the synthetic green rusts (Génin *et al.*, 1998; Bourrié *et al.*, 1999, 2004). Moreover, carbonate is known as an inhibitor of the formation of lepidocrocite (Schwertmann and Fechter, 1994). It was thus proposed that OH^- could be the interlayer anion. OH^- ions can be generated directly in the interlayer by deprotonation of water molecules when Fe^{2+} is oxidized, and there is no need to have OH^- ions present in the environment, only the possibility of protons diffusing out of the interlayer.

By letting $y = 0$, the pure ferroso-ferric end-member is $Fe_{1-x}^{2+}Fe_x^{3+}(OH)_{2+x}$; the upper limit for x is then 1/3, *i.e.* $Fe_3(OH)_7$ (point A, Figure 4a), and the lower limit is 1/4, *i.e.* $Fe_4(OH)_9$ (point M, Figure 4a). As more Mg enters the solid, a larger fraction of Fe can be oxidized, until all Fe is present as Fe^{3+}, which by letting $x = 1$ in the formula leads to a formula $Mg_2Fe_3^{3+}(OH)_{13}$, equivalent to pyroaurite with OH^- replacing CO_3^{2-} (point D, Figure 4a). 'Hydrated magnetite' $Fe_3O_4.nH_2O$ from Girard and Chaudron (1935), would be close to $Fe_3(OH)_8$, with $x = 2/3$, and can exist only with some Mg stabilizing the structure, *e.g.* as $MgFe_3(OH)_{10}$. The

domain of stability of hydroxy-fougerite is thus restricted to a thin band in the ternary system $Mg(OH)_2$–$Fe(OH)_2$–$Fe(OH)_3$ (Figure 4a, 4b). When extending the regular solid-solution model to other anions, it appears that soil solutions from Fougères are always undersaturated with respect to chloro-fougerite, always oversaturated with respect to hydroxy-fougerite, but either undersaturated or oversaturated with respect to carbonate-fougerite and sulfate-fougerite, depending on the Mg content and time (Feder *et al.*, 2005). As expected, Mg stabilizes the mineral. In Fougères, the *in situ* Mössbauer spectra showed that $1/3 \leqslant x \leqslant 2/3$; x is constant in straight lines issuing from the $Mg(OH)_2$ pole in the ternary diagram (dotted lines, Figure 4b). Microprobe analyses give a mole ratio of Mg/Fe_{total} in the range (0.18−0.62 − dashed horizontal lines, Figure 4b). By combining these data with the limits derived from the solid-solution model (solid lines, Figure 4b, Bourrié *et al.*, 2004), *Fougères*-fougerite can be constrained in the convex polygon obtained by the intersection of these six straight lines (Figure 4b).

Relation to other species

Fougerite is a layered double [Fe(II)-Fe(III)] or triple [Fe(II)-Mg(II)-Fe(III)] hydroxysalt, a member of the pyroaurite-iowaite group. The nature of the interlayer anion in *Fougères*-fougerite is probably OH^-, as derived from the chemical composition of the soil solutions and thermodynamic modeling of soil-solution equilibria. It could be different in other, less acidic environments. We can expect carbonate-fougerite to form in Gleysols on limestones, chloro-fougerite and sulfate-fougerite in lagoons or marshes influenced by sea salts. In particular, sulfate-fougerite could
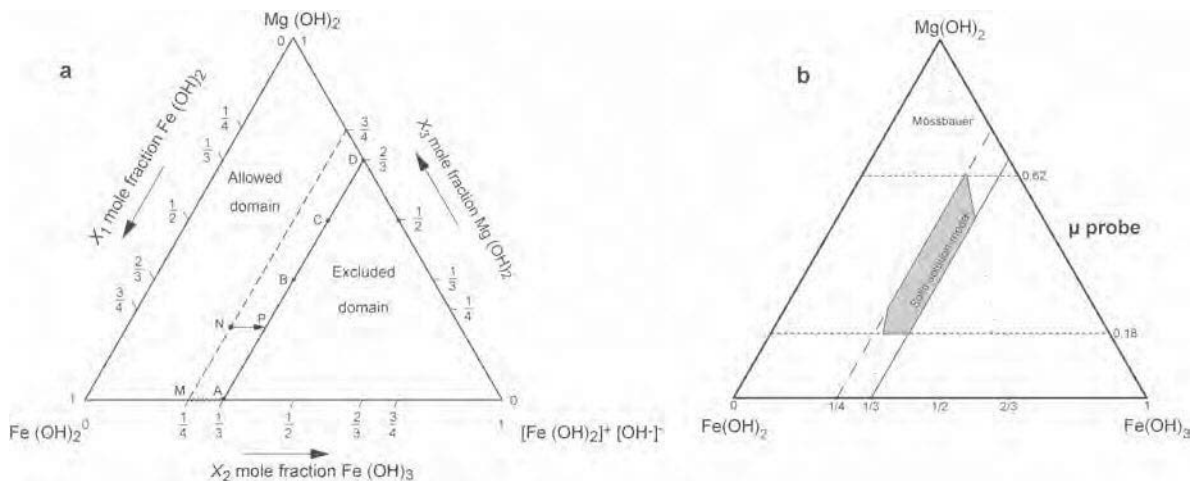

Figure 4. (a) Diagram for the ternary system $Mg(OH)_2$-$Fe(OH)_2$-$Fe(OH)_3$. Solid line: limit between the excluded domain and the domain allowed for stable 'green rusts' structure; dashed line: limit of the incipient precipitation of green rusts; from M to A on the horizontal axis: interval of the composition of synthetic green rusts; B, C and D: different compositions of green rusts; $N \to P$: oxidation path of fougerite. (b) Ternary diagram of the stability of fougerite derived from Mössbauer data (dotted lines), a solid-solution model (solid line and long dashed lines, see also Figure 4a), extraction by citrate-bicarbonate, and EMPA (horizontal short dashed lines). The limits of composition of fougerite from Fougères are given by the shaded area resulting from the intersections of those six straight lines.

form in acid sulfate soils, and possibly act as an intermediate phase to the formation of schwertmannite or Fe-jarosite during the oxidation of Fe sulfides.

Whatever the nature of the interlayer anion, because of the similarity between various crystal structures, each member of this group is related to layered hydroxycarbonates such as pyroaurite or hydrotalcite. This relationship was evident from the comparison of fougerite and synthetic Fe^{2+}-Fe^{3+}-Mg hydroxycarbonates by XAS and Mössbauer spectroscopies (Refait *et al.*, 2001). Fougerite is the Fe^{2+}-Fe^{3+}-dominant analogue of such hydroxysalts. Hydroxy-fougerite would be the Fe^{2+}-Fe^{3+}-dominant analogue of meixnerite (Koritnig and Süsse, 1975) and the Fe^{2+}-interlayer-OH-dominant analogue of iowaite (Kohls and Rodda, 1967; Braithwaite *et al.*, 1994). The proposed criteria to identify fougerite are summarized in Table 7.

Geochemical significance

Fougerite forms as easily as green rusts, and controls Fe in solution. In addition, Mg enters the mineral. In soils, the following genetic scheme has been proposed (Feder *et al.*, 2005): at the end of the dry season, the soil profile is completely oxidized with Fe present in the form of oxyhydroxides such as goethite or lepidocrocite. When reducing conditions appear, such as in autumn with both

a supply of organic matter and water saturation, Fe oxides are partly reduced and Fe^{2+} is released to solution. When oxygen enters the soil due to fluctuations of the water table or supplied by rainwater, Fe^{2+} is partly oxidized and fougerite forms by co-precipitation of Fe^{3+} with Fe^{2+} and Mg^{2+}. This is probably abiotic, as it is a fast phenomenon. In the field, with alternate moderately reducing to strongly reducing conditions, the *x* mole ratio fluctuates over time, and fougerite is subject to mineralogical transformations that can be monitored by *in situ* Mössbauer spectroscopy (Feder *et al.*, 2005). Oxidation of fougerite at constant Mg mole ratio ($N \rightarrow P$, Figure 4a) leads to an increase of the electrical charge of the layer. This can be simply compensated by a deprotonation of water molecules in the interlayer (Bourrié *et al.*, 2004) or by conversion of OH^- ions into O^{2-} ions in the hydroxide sheets (oxolation). For instance, it has been demonstrated that 'ferric GR', *i.e.* an Fe(III) compound with a layered structure similar to that of GRs, could be obtained under various conditions (Refait and Génin, 1993; Refait *et al.*, 2003; Legrand *et al.*, 2004). However, this compound shows a contraction of the *a* parameter that was not observed for fougerite. This sort of 'ferric GR' can be considered as a transient phase from fougerite to Fe oxyhydroxides. Eventually, fougerite is completely oxidized into lepidocrocite or goethite and Mg is released to

Table 7. Identification criteria proposed for fougerite and characteristics of hydroxy-fougerite.

Method	Criteria	
Color of soil or sediment	Bluish-green (Munsell 2.5 Y, 5 Y, 5 G, 5 B) turning to ochreous or reddish brown within a few hours of exposure to air	
Selective dissolution	Extractable by citrate-bicarbonate without the need for reduction by dithionite	
XRD	Main peak depending on the structure and the nature of the interlayer anion: GR1: system trigonal, space group $R\bar{3}m$ $d_{003} = 7.5-8$ Å depending on the nature of the interlayer anion; GR2: system trigonal, space group $P\bar{3}m1$ $d_{001} = 11.0-11.6$ Å for sulfate-fougerite with two planes interlayer (GR2). These values are close to the main peaks of kaolinite (7.13 Å) and interstratified clay minerals (10−14 Å), respectively, so that the identification may be difficult.	
Mössbauer spectroscopy	At 77−78 K, four doublets for GR1, two ferrous and two ferric D1: $\delta \approx 1.27$ mm s^{-1}; $\Delta E_Q \approx 2.86$ mm s^{-1} D2: $\delta \approx 1.25$ mm s^{-1}; $\Delta E_Q \approx 2.48$ mm s^{-1} D3: $\delta \approx 0.46$ mm s^{-1}; $\Delta E_Q \approx 0.48$ mm s^{-1} D4: $\delta \approx 0.46$ mm s^{-1}; $\Delta E_Q \approx 0.97$ mm s^{-1} Only two doublets for GR2, one ferrous and one ferric D1: $\delta \approx 1.27$ mm s^{-1}; $\Delta E_Q \approx 2.83$ mm s^{-1} D3: $\delta \approx 0.47$ mm s^{-1}; $\Delta E_Q \approx 0.45$ mm s^{-1} If silicated Fe is present, the distinction may be difficult.	
Raman spectroscopy	Bands at 427 and 518 cm^{-1}	
	Characteristics of hydroxy-fougerite	
Structural formula	$(Fe^{2+},Mg)_6Fe^{3+}_2(OH)_{18}\cdot 4H_2O$	$Z = 3/8$
System	Trigonal	Space group $R\bar{3}m$
Unit-cell	$a = 0.3125(5)$ nm $c \approx 2.256-2.385$ nm	$V \approx 0.19-0.20$ nm^3

The digits in parentheses are the one-standard-deviation uncertainty in the last digits of the given value.
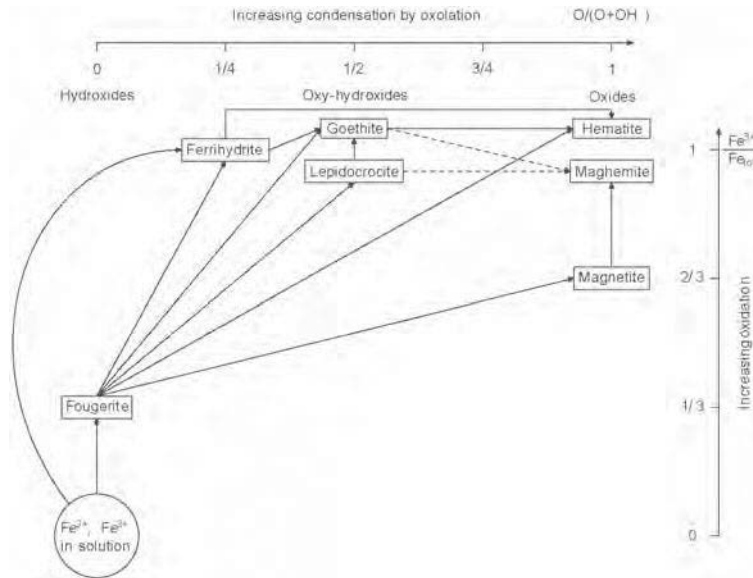
Figure 5. Location of fougerite in the pathways of formation of Fe oxides (*s.l.*). Abscissa: mole ratio O/(O+OH), increasing condensation by oxylation from left to right. Ordinate: mole ratio of Fe^{3+}/Fe_{total}, increasing oxidation from the bottom to the top. Fougerite and ferrihydrite appear as key intermediate phases.

solution. This can explain why Mg is present in exchangeable sites in oximorphic saprolite, while it is associated with Fe in reductomorphic saprolite and reductomorphic silty horizon. In addition to Fe, fougerite thus acts as a transient trap for Mg, linking Mg and Fe cycles.

In the scheme above, fougerite forms by an abiotic process, when oxygen enters the solution. However, bacterial activity can also lead to the formation of this mineral because biogenesis of GR from lepidocrocite reduction has been unambiguously observed (Ona-Nguema *et al.*, 2002; Zegeye *et al.*, 2005). Fougerite can thus form either by abiotic processes, by solution phase oxidation reactions, or by biotic process by reduction of Fe(III) oxides.

The compositions of Fe oxides (*s.l.*) differ by the Fe(III)/Fe$_{total}$ mole ratio and by the O/(O+OH) mole ratio. By considering the simultaneous variations of these ratios (Figure 5), it is possible to represent the pathways of formation of all Fe oxides. Fougerite and ferrihydrite appear as key intermediates in this diagram. Mild oxidation of aqueous Fe(II) leads to the formation of fougerite, while rapid oxidation leads to the formation of ferrihydrite.

Fougerite can act as an electron acceptor (*x* decreases) or an electron donor (*x* increases). Thermodynamic calculations show that the fougerite/ Fe^{2+} couple is active before the NO_3^-/NO_2^- couple (Trolard and Bourrié, 1999), so that fougerite reduction can compete with the first step of denitrification. In addition, fougerite can react directly with nitrate that is then reduced to ammonia (Hansen *et al.*, 1996; Huang and Zhang, 2004). These biotic and abiotic processes link the Fe and N cycles.

Moreover, fougerite, like other layered double hydroxides (Sparks, 2001; Peltier *et al.*, 2006), may react with silica and could play an essential role in the formation of clay minerals, including both phyllosilicates and Fe hydr(oxides) and in the control of both major elements (Mg, Fe), transition metals (Co, Cr, Mn, Ni and Zn) and noble metals (Ag, Au and Hg, Loughlin *et al.*, 2003) in the environment. The ability of fougerite to transform to ferric oxides or to react with silica to give clay minerals could explain the small size of fougerite crystals. Its domain of stability is narrow, and it is a transient phase.

ACKNOWLEDGMENTS

REFERENCES

Abdelmoula, M., Refait, Ph., Drissi, S.H., Mihe, J.-P. and Génin, J.-M.R. (1996) Conversion electron Mössbauer spectroscopy and X-ray diffraction studies of the formation

of carbonate-containing green rust one by corrosion of metallic iron in $NaHCO_3$ and ($NaHCO_3$ + NaCl) solutions. *Corrosion Science*, **38**, 623−663.

Abdelmoula, M., Trolard, F., Bourrié, G. and Génin, J.-M.R. (1998) Evidence for the Fe(II)-Fe(III) green rust 'fougerite' mineral and its transformation with depth. *Hyperfine Interactions*, **112**, 235−238.

Al-Agha, M.R., Burley, S.D., Curtis, C.D. and Esson, J. (1995) Complex cementation textures and authigenic mineral assemblages in recent concretions from the Lincolnshire Wash (east coast, UK) driven by Fe(0) to Fe(II) oxidation. *Journal of the Geological Society, London*, **152**, 157−171.

Allmann, R. (1968) The crystallographical structure of pyroaurite. *Acta Crystallographica*, **B24**, 972−977.

Allmann, R. (1970) Doppelschichtstrukturen mit brucitaehnlichen Schichtionen [Me(II)$_{1-x}$Me(III)$_x$ (OH)$_2$]$^{x+}$. *Chimia*, **24**, 99−108.

Aurousseau, P., Bourrié, G. and Curmi, P. (1987) Organisation, minéralogie et dynamique de l'aluminium dans les sols acides et pozoliques en climat tempéré et océanique (Exemples du Massif Armoricain, France). Pp. 85−105 in: *Table Ronde Internationale du CNRS, 'Podzols et Podzolisation'*, Poitiers, 10−11 April 1986, (D. Righi and A. Chauvel, editors), AFES-INRA, Paris.

Avery, B.W. (1973) Soil classification in the Soil Survey of England and Wales. *Journal of Soil Science*, **24**, 324−338.

Bernal, J.D., Dasgupta, D.T. and Mackay, L. (1959) The oxides and hydroxides of iron and their structural inter-relationships. *Clay Minerals Bulletin*, **4**, 15−30.

Bigham, J.K. and Tuovinen, O.H. (1985) Mineralogical, morphological, and microbiological characteristics of tubercles in cast iron water mains as related to their chemical activity. Pp. 239−250 in: *Planetary Ecology* (D.E. Caldwell, J.A. Brierley and C.L. Brierley, editors). Van Nostrand-Rheinold, Amsterdam, The Netherlands.

Bish, D.L. and Brindley, G.W. (1977) A reinvestigation of takovite, a nickel aluminum hydroxy-carbonate of the pyroaurite group. *American Mineralogist*, **62**, 458−464.

Boucherit, N., Hugot Le Goff, A. and Joiret, S. (1991) Raman studies of corrosion films grown on Fe and Fe-Mo in pitting conditions. *Corrosion Science*, **32**, 497−507.

Boucherit, N., Hugot-Le Goff, A. and Joiret, S. (1992) In situ Raman identification of stainless steels pitting corrosion films. *Material Sciences Forum*, **111−112**, 580−588.

Bourrié, G., Trolard, F., Génin, J.-M.R., Jaffrezic, A., Maître, V. and Abdelmoula, M. (1999) Iron control by equilibria between hydroxy-Green Rusts and solutions in hydromorphic soils. *Geochimica et Cosmochimica Acta*, **63**, 3417−3427.

Bourrié, G., Trolard, F., Refait, Ph. and Feder, F. (2004) A solid-solution model for Fe(II)-Fe(III)-Mg(II) green rusts and fougerite and estimation of their Gibbs free energies of formation. *Clays and Clay Minerals*, **52**, 382−394.

Braithwaite, R.S.W., Dunn, P.J., Pritchard, R.G. and Paar, W.H. (1994) Iowaite, a re-investigation. *Mineralogical Magazine*, **58**, 79−85.

Brindley, G.W. and Bish, D.L. (1976) Green rust: a pyroaurite type structure. *Nature*, **263**, 353.

Brindley, G.W. and Kikkawa, S. (1979) A crystal-chemical study of Mg, Al and Ni, Al hydroxy-perchlorates and hydroxy-carbonates. *American Mineralogist*, **64**, 836−843.

Drissi, S.H., Refait, Ph., Abdelmoula, M. and Génin, J.-M.R. (1995) Preparation and thermodynamic properties of Fe(II)-Fe(III) hydroxycarbonate (green rust 1), Pourbaix diagram of iron in carbonate-containing aqueous media. *Corrosion Science*, **37**, 2025−2041.

Duchaufour, Ph., Faivre, P. and Gury, M. (1976) *Atlas écologique des sols du monde*. Masson, Paris, p. 117.

Feder, F. (2001) Dynamique des processus d'oxydo-réduction dans les sols hydromorphes − Monitoring in situ de la solution du sol et des phases solides ferrifères. PhD thesis, Université d'Aix-Marseille III, Aix-en-Provence, France, 207 pp.

Feder, F., Trolard, F., Klingelhöfer, G. and Bourrié, G. (2005) In situ Mössbauer spectroscopy: evidence for green rust (fougerite) in a gleysol and its mineralogical transformations with time and depth. *Geochimica et Cosmochimica Acta*, **69**, 4463−4483.

Feitknecht, W. and Keller, G. (1950) Über die dunkelgrünen Hydroxyverbindungen des Eisens. *Zur Anorganische Allgemeine Chemie*, **262**, 61−68.

Génin, J.-M.R., Bourrié, G., Trolard, F., Abdelmoula, M., Jaffrezic, A., Refait, Ph., Maître, V., Humbert, B. and Herbillon, A. (1998) Thermodynamic equilibria in aqueous suspensions of synthetic and natural Fe(II)-Fe(III) Green Rusts: occurrences of the mineral in hydromorphic soils. *Environmental Science and Technology*, **32**, 1058−1068.

Génin, J.-M.R., Refait, Ph., Bourrié, G., Abdelmoula, M. and Trolard, F. (2001) Structure and stability of Fe(II)-Fe(III) green rust 'fougerite' mineral and its potential for reducing pollutants in soil solutions. *Applied Geochemistry*, **16**, 559−570.

Girard, A. and Chaudron, G. (1935) Sur la constitution de la rouille. *Comptes rendus de l'Académie des Sciences, Paris*, **200**, 127−129.

Hansen, H.C.B., Koch, C.B., Nancke-Krogh, H., Borggaard, O.K. and Sørensen, J. (1996) Abiotic nitrate reduction to ammmonium: key role of green rust. *Environmental Science and Technology*, **30**, 2053−2056.

Hashi, K., Kikkawa, S. and Koizumi, M. (1983) Preparation and properties of pyroaurite-like hydroxy minerals. *Clays and Clay Minerals*, **31**, 152−154.

Huang, Y.H. and Zhang, T.C. (2004) Effects of low pH on nitrate reduction by iron powder. *Water Research*, **38**, 2631−2642.

IUSS Working Group WRB (2006) *World reference base for soil resources 2006 − A framework for international classification, correlation and communication.* World Soil Resources Reports No. 103, FAO, Rome.

Koch, C.B. and Mørup, S. (1991) Identification of green rust in an ochre sludge. *Clay Minerals*, **26**, 577−582.

Kohls, D.W. and Rodda, J.L. (1967) Iowaite, a new hydrous magnesium hydroxide ferric oxychloride from the Precambrian of Iowa. *American Mineralogist*, **52**, 1261−1271.

Koritnig, S. and Süsse, P. (1975) Meixnerit, $Mg_6Al_2(OH)_{18}·4H_2O$, ein neues Magnesium-Aluminium-Hydroxid-Mineral. *Tschermaks Mineralogische und Petrographische Mitteilungen*, **22**, 79−87.

Legrand, L., Mazerolles, L. and Chaussé, A. (2004) The oxidation of carbonate green rust into ferric phases: solid-state reaction or transformation via solution. *Geochimica et Cosmochimica Acta*, **68**, 3497−3507.

Loughlin, E.J., Kelly, S.D., Kemner, K.M., Csencsits, R. and Cook, R.E. (2003) Reduction of Ag, Au^{III}, Cu^{II} and Hg^{II} by Fe^{II}/Fe^{III} hydroxysulfate green rust. *Chemosphere*, **53**, 437−446.

Mitchell, B.D., Smith, B.F.L. and Endredy, A.S. de (1971) The effect of buffered sodium dithionite solution and ultrasonic agitation on soil clays. *Israeli Journal of Chemistry*, **9**, 45−52.

Murad, E. and Taylor, R.M. (1986) The oxidation of hydroxycarbonate green rusts. Pp. 585−593 in: *Industrial Applications of the Mössbauer Effect* (G.J. Long and J.G. Stevens, editors). Plenum, New York.

Nguyen, Kha and Duchaufour, Ph. (1969) Note sur l'état du fer dans les sols hydromorphes. *Science du Sol*, 97−110.

Ona-Nguema, G., Abdelmoula, M., Jorand, F., Benali, O.,

Géhin, A., Block, J.C. and Génin, J.M.R. (2002) Iron (II,III) hydroxycarbonate green rust formation and stabilisation from lepidocrocite bioreduction. *Environmental Science and Technology*, **36**, 16−20.

Peltier, E., Allada, R.K., Navrotsky, A. and Sparks, D. (2006) Nickel solubility and precipitation in soils: a thermodynamic study. *Clays and Clay Minerals*, **54**, 153−164.

Ponnamperuma, F.N., Tianco, E.M. and Loy, T. (1967) Redox equilibria in flooded soils: I. The iron hydroxide system. *Soil Science*, **103**, 374−382.

Refait, Ph. and Génin, J.-M.R. (1993) The oxidation of Ni(II)-Fe(III) hydroxides in chloride-containing aqueous media. *Corrosion Science*, **34**, 2059−2070.

Refait, Ph., Abdelmoula, M. and Génin, J.-M.R. (1998a) Mechanisms of formation and structure of green rust one in aqueous corrosion of iron in the presence of chloride ions. *Corrosion Science*, **40**, 1547−1560.

Refait, Ph., Charton, A. and Génin, J.-M.R. (1998b) Identification, composition, thermodynamic and structural properties of a pyroaurite-like iron(II)-iron(III) hydroxy-oxalate Green Rust. *European Journal of Solid State Inorganic Chemistry*, **35**, 655−666.

Refait, Ph., Abdelmoula, M., Trolard, F., Génin, J.-M.R., Ehrhardt, J.J. and Bourrié, G. (2001) Mössbauer and XAS study of a green rust mineral; the partial substitution of Fe^{2+} by Mg^{2+}. *American Mineralogist*, **86**, 731−739.

Refait, Ph., Benali, O., Abdelmoula, M. and Génin, J.-M.R. (2003) Formation of 'ferric green rust' and/or ferrihydrite by fast oxidation of iron(II-III) hydroxychloride green rust. *Corrosion Science*, **45**, 2435−2449.

Roussel, H., Briois, V., Elkaim, E., de Roy, A. and Besse, J.P. (2000) Cationic order and structure of [Zn-Cr-Cl] and [Cu-Cr-Cl] layered double hydroxides: a XRD and EXAFS study. *Journal of Physical Chemistry*, **B25**, 5915−5963.

Schwertmann, U. and Fechter, H. (1994) The formation of green rust and its transformation to lepidocrocite. *Clay Minerals*, **29**, 87−92.

Simon, L., François, M., Refait, Ph., Renaudin, G., Lelaurain, M. and Génin, J.-M.R. (2003) Structure of the Fe(II-III) layered double hydroxysulphate green rust two from Rietveld analysis. *Solid State Sciences*, **5**, 327−334.

Sparks, D.L. (2001) Elucidating the fundamental chemistry of soils: past and recent achievements and future frontiers. *Geoderma*, **100**, 303−319.

Stampfl, P.P. (1969) Ein basisches Eisen-II-III-Karbonat in Rost. *Corrosion Science*, **9**, 185−187.

Taylor, H.F.W. (1973) Crystal structures of some double hydroxide minerals. *Mineralogical Magazine*, **39**, 377−389.

Taylor, R.M. (1981) Colour in soils and sediments − A review. Pp. 749−761 in: *International Clay Conference 1981*, Bologna-Pavia (H. van Olphen and F. Veniale, editors), Developments in Sedimentology, 35, Elsevier, Amsterdam.

Taylor, R.M. (1984) The rapid formation of crystalline double hydroxy salts and other compounds by controlled hydrolysis. *Clay Minerals*, **19**, 591−603.

Trolard, F. and Bourrié, G. (1999) L'influence des oxydes de fer de type 'rouilles vertes' sur les séquences d'oxydo-réduction dans les sols. *Comptes rendus de l'Académie des Sciences, Paris*, **329**, 801−806.

Trolard, F., Bourrié, G., Jeanroy, E., Herbillon, A. and Martin, H. (1995) Trace metals in natural iron oxides from laterites: a study using selective kinetic extractions. *Geochimica et Cosmochimica Acta*, **59**, 1285−1297.

Trolard, F., Abdelmoula, M., Bourrié, G., Humbert, B. and Génin, J.-M.R. (1996) Mise en évidence d'un constituant de type 'rouilles vertes' dans les sols hydromorphes − Proposition de l'existence d'un nouveau minéral: la 'fougérite'. *Comptes rendus de l'Académie des Sciences, Paris*, **323, série IIa**, 1015−1022.

Trolard, F., Génin, J.-M.R., Abdelmoula, M., Bourrié, G., Humbert, B. and Herbillon, A. (1997) Identification of a green rust mineral in a reductomorphic soil by Mössbauer and Raman spectroscopies. *Geochimica et Cosmochimica Acta*, **61**, 1107−1111.

Vysotskii, G.N. (1905) *Gley Pochvovedeniye*, **4**, 291−327 (original paper, in Russian). [1999] Gley. An abridged publication of Vysotskii 1905 on the 257th Anniversary of the Russian Academy of Sciences. *Eurasian Soil Science*, **32**, 1063−1068.

Zegeye, A., Ona-Nguema,G., Carteret, C., Huguet, L., Abdelmoula, M. and Jorand, F. (2005) Formation of hydroxysulphate green rust 2 as a single iron(II-III) mineral in microbial culture. *Geomicrobiology Journal*, **22**, 389−399.